A Data-driven quasi inverse static model of a parallel continuum robot

Seraphima S. B. Hanna[1*], A. M. M. Abdelhaleem[2], S. El-Naggar[2], Haitham El-Hussieny[3*]

Abstract— **Soft continuum robots, inspired by highly flexible biological structures such as octopus arms and elephant trunks, have attracted significant attention due to their inherent compliance and adaptability. Integrating soft continuum arms within a parallel kinematic architecture provides a promising solution to the traditional trade-off between dexterity and structural stiffness, combining the flexibility of soft robots with the precision and load-bearing capacity of rigid parallel mechanisms. However, deriving accurate and computationally efficient inverse models for such hybrid systems remains a major challenge, particularly for real-time control applications.**

This paper presents a novel data-driven inverse quasi-static modeling framework for a tendon-driven hybrid soft–rigid parallel robot. Unlike conventional forward statics models, the presented method focuses on learning the inverse relationship, mapping the target Cartesian coordinates of the end-effector to the tendon tension values necessary for actuation across the nine driving rods. A high-fidelity physics-based model implemented in the SoRoSim toolbox is employed to generate a comprehensive dataset under quasi-static conditions. This dataset is then utilized to train an artificial neural network (ANN) capable of approximating the highly nonlinear inverse relationship governing the system.

The predicted tension forces obtained from the ANN are systematically compared with the original SoRoSim-generated data to evaluate accuracy and generalization performance. Results demonstrate that the ANN achieves close agreement with the physics-based model while offering substantially reduced computational time, making it highly suitable for real-time implementation and control-oriented applications. The proposed framework establishes an efficient and scalable solution for inverse modeling of hybrid continuum parallel robots and provides a solid foundation for future closed-loop control and real-time trajectory tracking strategies.

Keywords— soft continuum robots, inverse quasi-static modeling, parallel robots, tendon-driven actuation, artificial neural networks, real-time control.

I. INTRODUCTION

In recent years, continuum robots have attracted increasing research attention, as reflected by the growing body of literature in this area [1]. These robotic systems are characterized by a highly flexible backbone [2], which allows continuous bending motions resulting from their elastic structural properties [3]. This inherent flexibility endows continuum robots with exceptional dexterity, maneuverability, and adaptability. As a result, these systems demonstrate exceptional suitability for deployment in restricted settings, where precise motion control and reliable human–robot safety are of paramount importance [4]. In contrast to traditional rigid-body robotic systems, continuum robots are capable of dynamically reconfiguring their shape, enabling effective navigation within complex and unstructured environments [5]. Owing to this distinctive versatility, continuum robots have been successfully applied across a broad range of domains, including industrial pipeline inspection [6], aircraft engine maintenance [7], and advanced medical and minimally invasive surgical procedures [8].

As a subclass of soft robotics, continuum robots feature a compliant continuous structure enabling smooth bending and torsional motions across multiple degrees of freedom [9]. Their applications extend to medical interventions [10], deep-sea exploration [11], and precision agriculture [12]. This adaptability highlights their suitability for tasks requiring flexibility, accuracy, and minimal invasiveness [13]. Soft robots differ from parallel robots by enabling deformation and biologically inspired motion absent in rigid mechanisms. Their compliance supports adaptability and safe interaction, proving effective in surgical robotics through enhanced minimally invasive procedures and surgeon feedback [14], [15]. They also aid rehabilitation via wearable exosuits offering customized assistance [16], and facilitate precise, low-force engagement in human–robot interaction [17]

Despite their advantages, continuum robots face key limitations. Low stiffness restricts force transmission, while complex actuation reduces accuracy and slows dynamics, particularly in elongated multi-DOF structures [18]. Trade-offs between flexibility and load capacity, along with nonlinear behaviors, intensive inverse kinematics, and singularity issues, further impair control precision and response time [19]. To address these constraints, research has increasingly focused on parallel continuum robots (PCRs). Here, multiple continuum arms are integrated into a common end-effector platform, markedly enhancing system rigidity [20]. Compared with single-chain designs, PCR kinematic chains are typically shorter and simpler, yielding higher accuracy and improved dynamics [21], [22]. While a single chain offers limited workspace, coordinated interaction among coupled robots, together with passive bending, enables more versatile motion of the overall system [21].

Sensitivity studies indicate that variations in tendon tension and segment design parameters directly affect stiffness and control precision, particularly in force-critical contexts such as surgical robotics [23]. For example,

[1*]Teaching Assistant, Department of Mechatronics, Higher Technological Institute,10th of Ramadan, Egypt.

Master Student, Department of Mechanical Design and Production specialty Mechatronics Engineering, Zagazig University, Egypt (e-mail: ss.hana23@eng.zu.edu.eg).

[2] Professor, Department of Mechanical Design and Production, Zagazig University, Egypt

[3*]Associate Professor, Department of Mechatronics and Robotics Engineering, Egypt-Japan University of Science and Technology (E-JUST), Alexandria, Egypt

(e-mail: haithm.elhussieny@ejust.edu.eg)

Böttcher, Lilge, and Burgner Kahrs (2021) showed that a tendon-driven PCR design achieved higher repeatability compared to individual continuum chains [24]. In this work, we propose a new spatial PCR architecture consisting of three tendon-actuated continuum robots connected via spherical joints to a common end-effector, as depicted in Fig. 1, 2.

Parallel robotic systems are recognized for their high stiffness and precise positioning, enabling them to sustain substantial loads while maintaining accurate motion control. These attributes have established them as essential in industrial automation, particularly in manufacturing and assembly where repeatable accuracy and dependable performance are critical [25]. Integrating soft robotics with parallel mechanisms combines complementary strengths to create versatile and efficient systems. This approach enhances positioning precision while preserving flexibility for complex tasks, opening opportunities in medical, industrial, and human-centered applications [26].

Numerous modeling strategies have been proposed for continuum robots, each based on specific assumptions and tailored to particular applications. A detailed overview and comparative assessment, including numerical formulations and practical aspects, is provided by Armanini [27]. Among these, the lumped mass model [28] represents a flexible link as discrete point masses connected by spring–damper elements. Each mass is influenced by gravity and neighboring dynamics, while selected masses may also experience external loads or actuator forces.

The piecewise constant curvature (PCC) model [29] simplifies continuum robot kinematics by approximating the structure as arc segments of uniform curvature. While computationally efficient, its constant-curvature assumption reduces accuracy when external effects such as gravity or friction are significant [30]. The discrete elastic rod (DER) model, introduced by Naughton et al. [31], provides a numerical framework for simulating slender, flexible structures. A continuous rod is discretized into interconnected segments, and discrete differential geometry captures bending and torsional deformations. While the DER approach balances computational cost and physical fidelity, it may not fully represent complex continuum robot architectures. Dynamic modeling of soft materials requires detailed consideration of kinematic, mechanical, and tribological effects, which the DER framework may not comprehensively address [32].

Figure 1 Hybrid parallel soft–rigid robotic system with three continuum actuators linked to a rigid upper platform via free joints, adapted from Nuelle et al. [33].

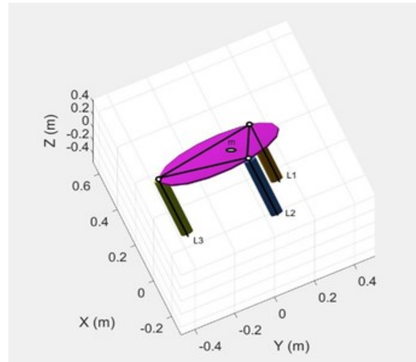

Figure 2. Kinematic representation of the hybrid parallel soft–rigid robot within the SoRoSim simulation framework. The rigid upper platform is connected to three soft continuum legs (L1–L3), each anchored to the base. This model serves as the basis for data generation and for validating the proposed ANN-based inverse statics methodology.

Finite-element modeling (FEM) has recently gained attention in soft robotics. These methods discretize the structure into one-, two-, or three-dimensional elements, following conventional robotic modeling approaches. Material deformation is analyzed using beam theories such as Euler–Bernoulli, Timoshenko, and Cosserat rod models [34]. While effective for small deformations [35], FEM suffers from drawbacks including high computational cost, sensitivity to instabilities, mesh distortion, and reduced reliability in large-deformation problems [36].

Although existing modeling strategies have advanced understanding of continuum robots, a critical gap persists in robust data-driven methods for statics modeling and control. This limitation restricts their broader adoption across applications. Data-driven frameworks, particularly machine learning, have been identified as promising, as noted by Wang et al. [1], [37]. With rapid progress in AI technologies—including neural networks, transformers, and generative models—the integration of data-driven statics modeling and control is especially compelling for soft continuum robots, offering improvements in accuracy, safety, and efficiency [38]. Simulation-based frameworks such as SoRoSim efficiently generate high-fidelity statics and kinematics data for complex soft–rigid architectures. Combining these outputs with data-driven methods, particularly artificial neural networks (ANNs), enables models that preserve physical accuracy while supporting real-time prediction and control. The following section outlines the methodology, including the spatial parallel continuum robot configuration, SoRoSim setup, and ANN-based inverse statics framework [39].

II. Methodology

A. *Parallel Tendon-driven Soft Continuum Robot Design*

The parallel soft robotic system investigated in this study comprises three identical soft links, each connected to a rigid end-effector platform through free joints. Each soft link is actuated by three tendon cables, resulting in a total of nine independent tension inputs. SoRoSim is a MATLAB-based toolbox developed for the modeling and analysis of hybrid rigid–soft robotic systems using the Geometric Variable-Strain (GVS) formulation [40]. This architecture facilitates the computational analysis of soft, rigid, and combined robotic structures, while incorporating Cosserat rod theory to capture bending, twisting, axial stretching, and shear deformations [41], [42].

To generate the dataset required for training the artificial neural network (ANN), the SoRoSim toolbox was utilized. A total of 2,000 data samples were produced by applying randomly selected tendon tension forces to the nine actuation cables of the parallel soft robot. The selected input variables are summarized in Table I and Table II, SoRoSim computed the corresponding end-effector position in Cartesian space (x,y,z) using the GVS-based modeling approach. The resulting workspace distribution of the tendon-driven parallel soft continuum robot, obtained from these randomized inputs, is illustrated in Fig. 3.

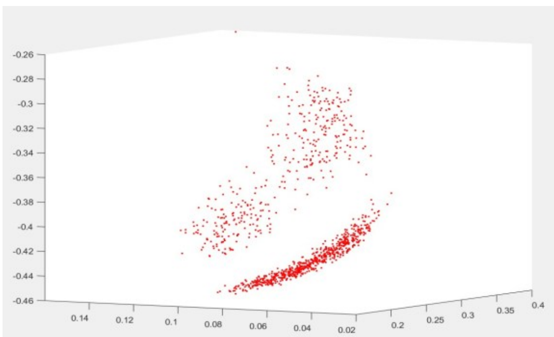

Figure 3. Workspace distribution of the parallel tendon-driven soft continuum robot. The three-dimensional scatter plot depicts the reachable end-effector positions obtained from SoRoSim simulations under randomly applied tendon tension inputs.

TABLE I. SoRoSim MODEL PARAMETERS OF THE SOFT ROBOTIC LINK

Parameter	**Value**	**Unit**	**Description**
Link Type	Soft ('s')	–	Type of link (soft or rigid)
Joint Type	Passive ('N')	–	Type of joint (active/passive)
Total Length	0.3	m	Overall length of the link
Number of Segments	2	–	Number of discrete segments
Young's	1×10^6	Pa	Material stiffness
Poisson's Ratio	0.5	–	Ratio of transverse to axial strain
Shear Modulus	3.33×10^5	Pa	Resistance to shear deformation
Internal Damping	10,000	–	Internal energy dissipation
Density	1000	kg/m^3	Mass per unit volume
Longitudinal Points	25	–	Discretization along the length
Radial Points	18	–	Discretization along the cross-section

Table 1. Parameters derived from the SoRoSim model implemented in MATLAB. The listed values correspond to the configuration of a single soft link within the parallel robotic architecture, including material properties, geometric characteristics, and discretization settings.

TABLE II. STRUCTURAL CONFIGURATION AND SIMULATION PARAMETERS OF THE PARALLEL SOFT ROBOT

Property	**Value**	**Description**
N	4	Number of links
ndof	15	Number of degrees of freedom
nsig	26	Number of signal variables
VLinks	1×4 SorosimLink	Array of soft link objects
LinkIndex	[1; 2; 3; 4]	Index of each link
CVTwists	4×1 cell	Cable twist data
lPre	[0; 0; 0; 0]	Initial pre-strain values
g_ini	16×4 double	Initial configuration matrix
Z_order	4	Z-axis ordering
nCLj	3	Number of closed-loop joints
iACL	[2; 3; 4]	Indices of actuated closed-loop joints
iCLB	[1; 1; 1]	Indices of base closed-loop joints
VTwistsCLj	1×3 SorosimTwist	Twist objects for closed-loop joints
gACLj, gBCLj	3×1 cell	Transformation matrices for joint frames
CLprecompute	1×1 struct	Precomputed closed-loop data
T_BS	0.0100	Time step for simulation
Gravity	0	Gravity setting (disabled)
G	0	Global stiffness (if applicable)
CEFP, M_added	0	Cable end force parameters and added mass
Actuated	1	Indicates actuation is enabled
nact	9	Number of actuators
Bqj1, iact	1	Actuation configuration indices

Table 2.Parameters obtained from the parallel_robot object in SoRoSim. The configuration includes three soft links and a single rigid link, together with closed-loop joint specifications, tendon routing information, and actuation parameters.

B. ANN-Based Static Modeling

To improve the efficiency of workspace prediction for the soft continuum robot, an artificial neural network (ANN) was trained using the previously generated simulation dataset. The ANN architecture, illustrated in Fig. 4, was designed to estimate the tendon actuation required to achieve a desired end-effector position. Specifically, the network predicts nine tendon tension values corresponding to the tendon-driven actuation system of the robot.

The proposed network consists of six layers in total. The input layer receives three continuous-valued variables representing the Cartesian coordinates (x,y,z) of the center of the robot's end-effector platform. This is followed by four fully connected hidden layers comprising 40, 30, 20, and 9 neurons, respectively. The hidden layers employ a combination of Rectified Linear Unit (ReLU) and Sigmoid activation functions, which are selected to introduce nonlinearity and enhance the model's generalization capability across complex input–output relationships. This architectural design enables the ANN to capture the highly nonlinear mapping between the desired end-effector position and the corresponding tendon tension distribution.

The output layer consists of nine neurons, each representing a predicted tendon tension value. These outputs define the set of tendon forces that must be applied to the nine tendon cables in order to position the center of the rigid platform at the desired spatial location.

For reliable learning and objective assessment of the proposed model, the available dataset was systematically divided into three subsets. Specifically, 70% of the samples were allocated for network training, while the remaining data were evenly distributed between validation and testing phases (15% each). This splitting strategy ensures balanced representation of the workspace across all subsets, supporting stable learning behavior and reducing the risk of model bias, overfitting, or insufficient generalization.

III. Results & Discussion

A. Model Accuracy and Training Evaluation

The proposed artificial neural network demonstrated stable convergence behavior during the training phase. As shown in Fig. 5, the validation mean squared error (MSE) reached 0.62467 at epoch 62, with the training and validation loss curves gradually approaching one another over successive epochs. This consistent convergence indicates steady optimization and balanced learning, without evident signs of overfitting or instability. The training evolution further confirms that the ANN effectively learned the nonlinear inverse mapping between the Cartesian coordinates (x,y,z) of the platform center and the corresponding tendon tension forces applied through the nine actuation cables. Overall, the network maintained satisfactory stability and predictive consistency throughout the training process.

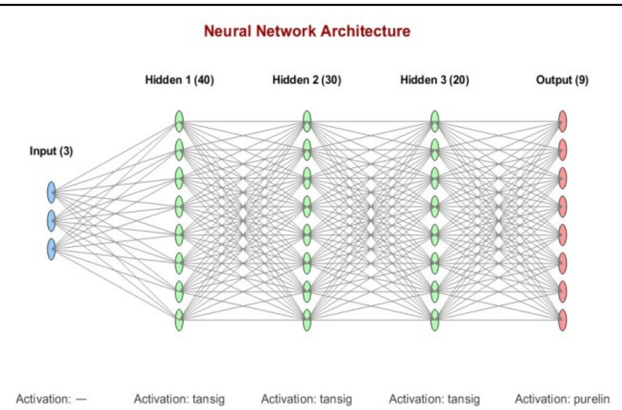

Figure 4. Architecture of the artificial neural network (ANN) employed for inverse statics modeling. The network maps the desired end-effector Cartesian position (x, y, z) to the corresponding set of nine tendon tension values required to achieve the specified platform configuration.

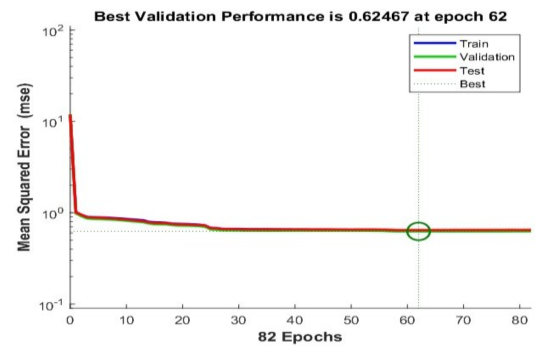

Figure 5. Training and validation loss curves of the proposed ANN model. The progressive convergence of both curves, reaching a validation MSE of 0.62467 at epoch 62, demonstrates stable optimization behavior and consistent generalization performance without significant divergence between training and validation errors.

B. Model-SoRoSim Comparison and Accuracy Analysis

A direct quantitative and visual comparison between the outputs predicted by the artificial neural network and those generated using the SoRoSim simulation framework further demonstrates the robustness and predictive reliability of the proposed model. As illustrated in Fig. 6, the Cartesian coordinates estimated by the ANN exhibit a strong agreement with the corresponding positions computed

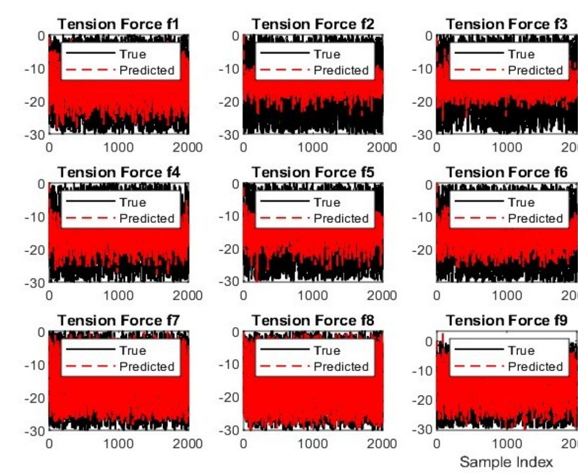

Figure 6. Correlation between the nine tendon tension forces estimated by the ANN and the corresponding values obtained from the SoRoSim-based GVS model.

through SoRoSim. The plotted results reveal an almost linear distribution along the reference line, indicating minimal deviation between predicted and simulated values across the evaluated dataset. Additionally, the average computation time over 100 samples was measured, yielding 0.256 s for SoRoSim (standard deviation: 0.470 s) and 0.014 s for the ANN (standard deviation: 0.007 s). This strong agreement underscores the effectiveness of the data-driven model in faithfully reproducing the nonlinear relationship initially defined by the Geometric Variable-Strain (GVS) formulation. Despite the inherent complexity of the GVS-based statics computation, the ANN effectively reproduces its behavior with high fidelity. At the same time, the neural-network-based approach offers a significant computational advantage, as it enables rapid prediction once trained, thereby enhancing efficiency compared to iterative simulation-based evaluations.

C. Prospective Enhancement and Research Trajectories

Further improvements in model performance can be achieved through structured optimization and architectural refinement. A primary direction involves systematic hyperparameter tuning, including careful adjustment of learning rates and the implementation of appropriate regularization techniques to further reduce residual prediction errors and enhance convergence stability. In addition, exploring alternative activation functions or advanced architectural configurations—such as residual connections or dropout layers—may improve generalization capability and mitigate overfitting, particularly when dealing with complex and non-uniform input distributions.

Moreover, the integration of convolutional neural networks (CNNs) or hybrid learning frameworks could significantly enhance the representational capacity of the model, especially in dynamic scenarios where capturing spatio-temporal dependencies is essential. Such developments would be particularly valuable in future research aimed at real-time path planning, adaptive control strategies, and multi-objective optimization of continuum robotic systems.

IV. Conclusion

This paper introduced a data-driven inverse quasi-static modeling framework for a hybrid soft–rigid parallel robot. The proposed approach employed an artificial neural network (ANN) to approximate the inverse kinematics mapping between the desired end-effector pose and the corresponding actuator inputs. The training dataset was generated using the physics-based mathematical model implemented in the SoRoSim toolbox, enabling the neural network to learn the nonlinear behavior of the continuum structure under quasi-static conditions.A comparative analysis between the ANN-based model and the original mathematical formulation demonstrated that the neural network achieves comparable accuracy while significantly reducing computational time. This reduction in computational complexity makes the proposed inverse model particularly suitable for real-time implementation, where rapid and reliable estimation of actuator commands is essential.The results confirm that integrating data-driven techniques with physics-based simulation tools provides an efficient alternative to purely analytical inverse models for complex soft robotic systems. The developed framework establishes a solid foundation for future work on closed-loop control, adaptive strategies, and real-time trajectory tracking of hybrid continuum parallel robots.

References

[1] Z. Chen *et al.*, ‘Data-driven Methods Applied to Soft Robot Modeling and Control: A Review’, *IEEE Trans. Autom. Sci. Eng.*, vol. 22, pp. 2241–2256, 2025, doi: 10.1109/TASE.2024.3377291.
[2] H. Wang, Y. Mao, and J. Du, ‘Continuum Robots and Magnetic Soft Robots: From Models to Interdisciplinary Challenges for Medical Applications’, *Micromachines*, vol. 15, no. 3, p. 313, Feb. 2024, doi: 10.3390/mi15030313.
[3] C. Alessi, C. Agabiti, D. Caradonna, C. Laschi, F. Renda, and E. Falotico, ‘Rod models in continuum and soft robot control: a review’, Jul. 08, 2024, *arXiv*: arXiv:2407.05886. doi: 10.48550/arXiv.2407.05886.
[4] I. A. Seleem, H. El-Hussieny, and H. Ishii, ‘Imitation-Based Motion Planning and Control of a Multi-Section Continuum Robot Interacting With the Environment’, *IEEE Robot. Autom. Lett.*, vol. 8, no. 3, pp. 1351–1358, Mar. 2023, doi: 10.1109/LRA.2023.3239306.
[5] I. Magomedov, T. Aygumov, and F. Dzamikhova, ‘Continuum robotics: Variations, applications, and limitations’, *ITM Web Conf.*, vol. 72, p. 02010, 2025, doi: 10.1051/itmconf/20257202010.
[6] M. Wooten, C. Frazelle, I. D. Walker, A. Kapadia, and J. H. Lee, ‘Exploration and Inspection with Vine-Inspired Continuum Robots’, in *2018 IEEE International Conference on Robotics and Automation (ICRA)*, Brisbane, QLD: IEEE, May 2018, pp. 5526–5533. doi: 10.1109/ICRA.2018.8461132.
[7] T. Pang, J. Liang, Z. Lin, X. Zhang, and F. Du, ‘Enhancing the precision of continuum robots in orthopedic surgery based on mechanical principles’, *Front. Bioeng. Biotechnol.*, vol. 12, Oct. 2024, doi: 10.3389/fbioe.2024.1470069.
[8] Y. Cao *et al.*, ‘Continuum robots for endoscopic sinus surgery: Recent advances, challenges, and prospects’, *Int. J. Med. Robot.*, vol. 19, no. 2, Apr. 2023, doi: 10.1002/rcs.2471.
[9] Ji, K.; Fang, Y., ‘A Review of Continuum Robot’, *Appl. Comput. Eng.*, vol. 36, 2024.
[10] H. Liu, ‘Recent advances on application of continuum robots in minimally invasive surgery’, *Appl. Comput. Eng.*, vol. 71, no. 1, pp. 72–77, Aug. 2024, doi: 10.54254/2755-2721/71/20241630.
[11] G. Li *et al.*, ‘Bioinspired soft robots for deep-sea exploration’, *Nat. Commun.*, vol. 14, no. 1, Nov. 2023, doi: 10.1038/s41467-023-42882-3.
[12] H. Wang, J. Du, and Y. Mao, ‘Hydrogel-Based Continuum Soft Robots’, *Gels*, vol. 11, no. 4, p. 254, Mar. 2025, doi: 10.3390/gels11040254.
[13] R. V. S, A. Rajesh, M. I. A. Athaaillah, and G. Prabhakar, ‘Serpentine Synergy: Design and Fabrication of a Dual Soft Continuum Manipulator and Soft Snake Robot’, Jul. 05, 2024, *arXiv*: arXiv:2407.04802. doi: 10.48550/arXiv.2407.04802.
[14] J. Zhu *et al.*, ‘Intelligent Soft Surgical Robots for Next-Generation Minimally Invasive Surgery’, *Adv. Intell. Syst.*, vol. 3, no. 5, May 2021, doi: 10.1002/aisy.202100011.
[15] T. Kong *et al.*, ‘Advances in Magnetically Controlled Medical Robotics: A Review of Actuation Systems, Continuum Designs, and Clinical Prospects for Minimally Invasive Therapies’,

Micromachines, vol. 16, no. 5, p. 561, May 2025, doi: 10.3390/mi16050561.
[16] N. Tanczak *et al.*, 'Soft Robotics in Upper Limb Neurorehabilitation and Assistance: Current Clinical Evidence and Recommendations', *Soft Robot.*, Dec. 2024, doi: 10.1089/soro.2024.0034.
[17] D. L. Cordon, S. Moss, M. Killpack, and J. L. Salmon, 'Leveraging Passive Compliance of Soft Robotics for Physical Human-Robot Collaborative Manipulation', Apr. 11, 2025, *arXiv*: arXiv:2504.08184. doi: 10.48550/arXiv.2504.08184.
[18] Y. Fan, B. Yi, and D. Liu, 'An overview of stiffening approaches for continuum robots', *Robot. Comput.-Integr. Manuf.*, vol. 90, p. 102811, Dec. 2024, doi: 10.1016/j.rcim.2024.102811.
[19] Y. Sun and S. Wang, 'An Optimization-Based Inverse Kinematics Solver for Continuum Manipulators in Intricate Environments', Oct. 27, 2024, *arXiv*: arXiv:2410.20311. doi: 10.48550/arXiv.2410.20311.
[20] S. Lilge, T. D. Barfoot, and J. Burgner-Kahrs, 'State Estimation for Continuum Multi-Robot Systems on SE(3)', Dec. 02, 2024, *arXiv*: arXiv:2401.13540. doi: 10.48550/arXiv.2401.13540.
[21] janabi-S. Jalali, Amir Farrokh, 'Dynamic Manipulation and Stiffness Modulation of Cooperative Continuum Robots: Theory and Experiment', 2024. doi: 10.1115/1.4064815.
[22] M. Russo, N. Sriratanasak, W. Ba, X. Dong, A. Mohammad, and D. Axinte, 'Cooperative Continuum Robots: Enhancing Individual Continuum Arms by Reconfiguring Into a Parallel Manipulator', *IEEE Robot. Autom. Lett.*, vol. 7, no. 2, pp. 1558–1565, Apr. 2022, doi: 10.1109/lra.2021.3139371.
[23] K. Sawant, A. E. Gkikakis, and L. S. Mattos, 'Investigating the Stiffness Characteristics of a Tendon-Driven Continuum Manipulator Using Sensitivity Analysis: A Case Study in Transoral Laser Microsurgery', *Machines*, vol. 11, no. 6, p. 662, Jun. 2023, doi: 10.3390/machines11060662.
[24] G. Boettcher, S. Lilge, and J. Burgner-Kahrs, 'Design of a Reconfigurable Parallel Continuum Robot With Tendon-Actuated Kinematic Chains', *IEEE Robot. Autom. Lett.*, vol. 6, no. 2, pp. 1272–1279, Apr. 2021, doi: 10.1109/lra.2021.3057557.
[25] M. Deja and A. P. Markopoulos, 'Advances and Trends in Non-Conventional, Abrasive and Precision Machining', *Machines*, vol. 9, no. 2, p. 37, Feb. 2021, doi: 10.3390/machines9020037.
[26] M. R. Montero, E. Shahabi, G. Franzese, J. Kober, B. Mazzolai, and C. D. Santina, 'Mastering Contact-rich Tasks by Combining Soft and Rigid Robotics with Imitation Learning', Oct. 11, 2024, *arXiv*: arXiv:2410.07787. doi: 10.48550/arXiv.2410.07787.
[27] C. Armanini, F. Boyer, A. T. Mathew, C. Duriez, and F. Renda, 'Soft Robots Modeling: A Structured Overview', *IEEE Trans. Robot.*, vol. 39, no. 3, pp. 1728–1748, Jun. 2023, doi: 10.1109/tro.2022.3231360.
[28] H. Habibi *et al.*, 'Modelling an Actuated Large Deformation Soft Continuum Robot Surface Undergoing External Forces Using a Lumped-Mass Approach', in *2018 IEEE/RSJ International Conference on Intelligent Robots and Systems (IROS)*, Madrid, Spain: IEEE, Oct. 2018, pp. 5958–5963. doi: 10.1109/iros.2018.8594033.
[29] I. A. Seleem, S. F. M. Assal, H. Ishii, and H. El-Hussieny, 'Demonstration-Guided Pose Planning and Tracking for Multi-Section Continuum Robots Considering Robot Dynamics', *IEEE Access*, vol. 7, pp. 166690–166703, 2019, doi: 10.1109/access.2019.2953122.
[30] F. Stella, Q. Guan, J. Leng, C. D. Santina, and J. Hughes, 'Piecewise Affine Curvature model: a reduced-order model for soft robot-environment interaction beyond PCC', Nov. 18, 2022, *arXiv*: arXiv:2211.10188. doi: 10.48550/arXiv.2211.10188.
[31] N. Naughton, J. Sun, A. Tekinalp, G. Chowdhary, and M. Gazzola, 'Elastica: A compliant mechanics environment for soft robotic control', Sep. 17, 2020, *arXiv*: arXiv:2009.08422. doi: 10.48550/arXiv.2009.08422.
[32] A. Choi, R. Jing, A. Sabelhaus, and M. K. Jawed, 'DisMech: A Discrete Differential Geometry-based Physical Simulator for Soft Robots and Structures', *IEEE Robot. Autom. Lett.*, vol. 9, no. 4, pp. 3483–3490, Apr. 2024, doi: 10.1109/LRA.2024.3365292.
[33] K. Nuelle and others, 'Modeling, calibration, and evaluation of a tendon-actuated planar parallel continuum robot', *IEEE Robot. Autom. Lett.*, vol. 5, no. 4, pp. 5811–5818, 2020.
[34] S. M. H. Sadati *et al.*, '*TMTDyn*: A Matlab package for modeling and control of hybrid rigid–continuum robots based on discretized lumped systems and reduced-order models', *Int. J. Robot. Res.*, vol. 40, no. 1, pp. 296–347, Jan. 2021, doi: 10.1177/0278364919881685.
[35] I. A. Gravagne, C. D. Rahn, and I. D. Walker, 'Large deflection dynamics and control for planar continuum robots', *IEEEASME Trans. Mechatron.*, vol. 8, no. 2, pp. 299–307, Jun. 2003, doi: 10.1109/tmech.2003.812829.
[36] H. Chen *et al.*, 'Accelerated Quasi-Static FEM for Real-Time Modeling of Continuum Robots with Multiple Contacts and Large Deformation', Mar. 10, 2025, *arXiv*: arXiv:2503.06922. doi: 10.48550/arXiv.2503.06922.
[37] H. Liu, 'A Survey on Application of Data-driven Model Predictive Control in Robot Control', 2025.
[38] H. A. Pierson and M. S. Gashler, 'Deep learning in robotics: a review of recent research', *Adv. Robot.*, vol. 31, no. 16, pp. 821–835, Aug. 2017, doi: 10.1080/01691864.2017.1365009.
[39] M. Kasaei, F. Alambeigi, and M. Khadem, 'A Synergistic Framework for Learning Shape Estimation and Shape-Aware Whole-Body Control Policy for Continuum Robots', Feb. 20, 2025, *arXiv*: arXiv:2501.03859. doi: 10.48550/arXiv.2501.03859.
[40] A. T. Mathew, I. B. Hmida, C. Armanini, F. Boyer, and F. Renda, 'SoRoSim: A MATLAB Toolbox for Hybrid Rigid–Soft Robots Based on the Geometric Variable-Strain Approach', *IEEE Robot. Autom. Mag.*, vol. 30, no. 3, pp. 106–122, Sep. 2023, doi: 10.1109/MRA.2022.3202488.
[41] A. T. Mathew, I. B. Hmida, C. Armanini, F. Boyer, and F. Renda, 'SoRoSim: A MATLAB Toolbox for Hybrid Rigid–Soft Robots Based on the Geometric Variable-Strain Approach', *IEEE Robot. Autom. Mag.*, vol. 30, no. 3, pp. 106–122, Sep. 2023, doi: 10.1109/mra.2022.3202488.
[42] H. Jiang *et al.*, 'Design, Control, and Applications of a Soft Robotic Arm', Jul. 08, 2020, *arXiv*: arXiv:2007.04047. doi: 10.48550/arXiv.2007.04047.